SH2B1β enhances fibroblast growth factor 1 (FGF1)-induced neurite outgrowth through MEK-ERK1/2-STAT3-Egr1 pathway

Wei-Fan Lin [a], Chien-Jen Chen [a,1], Yu-Jung Chang [a,1], Su-Liang Chen [d], Ing-Ming Chiu [d,e], Linyi Chen [a,b,c,*]

[a] *Institute of Molecular Medicine, National Tsing Hua University, Hsinchu, Taiwan*
[b] *Department of Life Science, National Tsing Hua University, Hsinchu, Taiwan*
[c] *Brain Research Center, National Tsing Hua University, Hsinchu, Taiwan*
[d] *Institute of Cellular and System Medicine, National Health Research Institutes, Miaoli, Taiwan*
[e] *Department of Internal Medicine, The Ohio State University, Columbus, OH, USA*

ARTICLE INFO

ABSTRACT

Genetic studies have established the crucial roles of FGF signaling, FGF-induced gene expression and morphogenesis during embryogenesis. In this study, we showed that overexpressing a signaling adaptor protein, SH2B1β, enhanced FGF1-induced neurite outgrowth in PC12 cells. SH2B1β has previously been shown to promote nerve growth factor (NGF) and glial cell line-derived neurotrophic factor (GDNF)-induced neurite outgrowth, in part, through prolonging NGF and GDNF-induced signaling. To delineate how SH2B1β promotes FGF1-induced neurite outgrowth, we examined its role in FGF1-dependent signaling. Our data suggest that SH2B1β enhances and prolongs FGF1-induced MEK-ERK1/2 and PI3K-AKT pathways. We also provided the first evidence that FGF1 induces the phosphorylation of signal transducer and activator of transcription 3 (STAT3) at serine 727 [pSTAT3(S727)] in PC12 cells. SH2B1β enhances this phosphorylation and the expression of the immediate early gene, Egr1. Through inhibitor assays, we have further shown that MEK-ERK1/2 is required for FGF1-induced neurite outgrowth, pSTAT3(S727) and Egr1 expression. Moreover, inhibiting Rho kinase, ROCK, enhances FGF1-induced neurite outgrowth through pSTAT3(S727)-independent manner. Taken together, our results demonstrate, for the first time, that SH2B1β enhances FGF1-induced neurite outgrowth in PC12 cells mainly through MEK-ERK1/2-STAT3-Egr1 pathway.

© 2009 Elsevier Inc. All rights reserved.

1. Introduction

Fibroblast growth factors (FGFs) are involved in the regulation of many developmental processes including patterning, morphogenesis, differentiation, proliferation and migration [1–12]. Such a diverse array of activities requires complex control of the signal transduction and the downstream transcriptional activity. FGF signaling is essential for the embryonic development as well as adult homeostasis of almost all the tissues/organs including neural induction, midbrain–hindbrain patterning, limb induction and morphogenesis, and skeletal development for various species [13–21]. Several studies have led to the dogma of which bone morphogenesis proteins (BMPs) expressed in the ectoderm inhibit the neural fate and this inhibition is relieved by FGF, suggesting a role of FGF in neural induction in chick [22–24]. FGFs represent a family of secreted molecules that are fairly conserved over evolution. In invertebrates, three FGFs are found in *Drosophila* while two are found in *Caenorhabditis elegans* so far. In vertebrates, a large number of FGF genes have been identified: 10 in Zebrafish, 6 in *Xenopus*, 13 in chicken, 22 in mouse and human [25]. All FGFs share a similar structure of internal core and high affinity for heparin. FGFs initiate their action through binding to FGF receptors (FGFRs), members of the receptor tyrosine kinases RTKs. FGFRs contain three immunoglobulin (Ig)-like domains and a heparin-binding sequence. FGF-FGFR interaction and signaling are further regulated by the spatial and temporal expression of heparan sulfate proteoglycan (HSPG). HSPGs are cell-surface and extracellular matrix macromolecules that comprise a core protein to which heparan sulfate (HS) glycosaminoglycan (GAG) chains are attached. HSPGs play crucial role in regulating multiple developmental pathways such as the FGF signaling (for review, [26]). It has been shown that HSPGs interact with FGFs and their receptors in a ternary complex at the cell surface and are required for FGF to elicit its effect during development [27–30]. Homodimerization of FGFRs leads to tyrosine phosphorylation at its cytoplasmic domain. Activation of FGFR allows for the recruitment and activation of Src homology (SH2)- or phosphotyrosine (PTB)-containing proteins, leading to the activation of various cytoplasmic signal transduction pathways. These pathways include those involve phospholipase C-γ (PLCγ), FGFR substrate 2α (FRS2α)-Ras/extracellular signal-regulated kinase (ERK) and phosphoinositol-3-

kinase (PI3K)-AKT pathways [31–36]. FGFR1, 2 and 3 are expressed differentially in subsets of neurons within the peripheral nervous system (PNS) and the central nervous system (CNS) [37–40].

SH2B1, an adapter/scaffold protein, belongs to a family of adapter proteins including APS (SH2B2) and Lnk (SH2B3) [41,42]. SH2B1 family members contain three proline-rich domains, a pleckstrin homology (PH) domain and a C-terminal Src homology (SH2) domain. The four known SH2B1 splice variants, α, β, γ, and δ, differ only in their C-termini starting just past the SH2 domain [43]. SH2B1α and β have been shown to bind to the activated nerve growth-activated factor (NGF) receptor TrkA through its SH2 domain and promote NGF-induced neurite outgrowth [44,45]. NGF promotes the rapid association of SH2B1β with TrkA and subsequent phosphorylation of SH2B1β on tyrosines as well as serines/threonines. Overexpression of SH2B1α or SH2B1β enhances NGF-induced neurite outgrowth in PC12 cells [44,46]. In additional to NGF signaling, SH2B1β has recently been shown to shuttle between the cytoplasm and the nucleus, attesting its novel function in transcriptional regulation [47]. Along this line, a recent study has revealed new function of SH2B1β in regulating the expression of a subset of NGF-responsive genes as well as the three-dimensional neurite outgrowth [48]. In addition to regulating NGF, the interaction of SH2B1β and RET receptor has been implicated in promoting glia-derived growth factor (GDNF)-induced neurite outgrowth [49].

Our primary interest is to determine the role that SH2B1β plays in FGF1-induced neurite outgrowth. In this study, we set out to determine whether SH2B1β affects FGF1-induced signaling, including MEK-ERK1/2 and PI3K-AKT pathways. We also examined whether SH2B1β plays a role in regulating the downstream transcription factor and gene expression of FGF1 signaling. Furthermore, we used SH2B1β mutants to determine what domains of SH2B1β contribute to its enhancing ability in FGF1-induced neurite outgrowth.

2. Materials and methods

2.1. Antibodies and reagents

Polyclonal antibody to rat SH2B1β was raised against a glutathione S-transferase fusion protein containing amino acids 527–670 of SH2B1β as described previously [42] and was used at a dilution of 1:15000 for Western blotting. Anti-ERK1/2 was from Sigma and was used at a dilution of 1:20000 for Western blotting. Anti-pERK1/2 (Thr202, Tyr204), anti- STAT3 and anti-pSTAT3(Ser727) were from Cell Signaling (Danvers, MA) and were used at a dilution of 1:2000. Anti-AKT, anti-pAKT(Ser473) and ant-pAKT(Thr308) were from Cell Signaling and were used at a dilution of 1:1000 for Western blotting. Anti-Egr1 and anti-p35 were purchased from Santa Cruz (Santa Cruz, CA) and were used at a dilution of 1:1000 and 1:200 respectively for Western blotting. Neuronal β-tubulin (TuJ1) was from Covance (Richmond, CA) and was used at a dilution of 1:1000 for immunofluorescence staining. Anti-rabbit Alexa Fluor 680 and anti-mouse Alexa Fluor 594 were from Invitrogen (Carlsbad, CA). NGF, rat-tail collagen I, and growth factor-reduced Matrigel were purchased from BD Bioscience. Human FGF1 (R1001) was purchased from Chingen Inc. (Dublin, Ohio) and heparin was purchased from Sigma. U0126, LY294002 and Y-27632 were from Calbiochem. Power SYBR® green PCR master mix and high capacity cDNA reverse transcription kit were from Applied Biosystems, Taiwan. TRIzol reagent was from Invitrogen (Carlsbad, CA). Protein Assay Kit (PAK500) was purchased from Strong Biotech Corporation, Taiwan.

2.2. Stable cell lines and cell culture

The stock of PC12 cells was purchased from American Type Culture Collection. PC12 cells were maintained on the collagen-coated plates (coated with 0.1 mg/ml rat-tail collagen in 0.02 N acetic acid) and grown at 37 °C in 10% CO_2 in complete media, DMEM (Invitrogen) supplemented with 10% heat-inactivated horse serum (16050-122, Invitrogen), 5% fetal bovine serum (26140-079, Invitrogen), 1 mM L-glutamine and 1 mM antibiotic-antimycotic (Invitrogen). PC12 cells stably overexpressing GFP, GFP-SH2B1β, GFP-SH2B1β(R555E), GFP-SH2B1β(270–670) or GFP-SH2B1β(397–670) were made and cultured as described in Chen et al [47]. Pooled population of stable clones was used to avoid clonal variation.

2.3. Neurite outgrowth

For FGF1-induced neurite outgrowth, PC12 cells were split onto 1:100 Matrigel-coated six-well plates at about 30% confluency. Culture medium was changed to low-serum differentiation media (DMEM containing 2% horse serum, 1% fetal bovine serum, 1% antibiotic-antimycotic and 1% L-glutamine) the next day. Cells were pre-treated 1 h with or without 20 μM of U0126, LY294002 or 10 μM Y-27632 before the addition of 100 ng/ml FGF1 and 10 μg/ml heparin. Neurite outgrowth was monitored for 6 days. Medium containing FGF1 and the inhibitor was replaced every two days. Images of differentiating cells were taken using inverted Zeiss Axiover 135 fluorescence microscope. The established definition of morphological differentiation in PC12 cells is that the length of the neurite should be at least twice of the diameter of the cell body. The percentage of differentiation was scored as the percentage of differentiated cells per counted cells.

2.4. RNA preparation and semi-quantitative real-time PCR

TRIzol reagent was use to isolate total RNA form PC12 cells with or without treatment at the indicated time. Concentration and $A_{260/280}$ ratio of RNAs were measured using spectrophotometer (NanoDrop 1000, Themo). Total RNA of each sample was reverse transcribed into cDNA and the relative gene expression of Egr1, p35 and glyceraldehydes-3-phosphate dehydrogenase (GAPDH) was determined via semi-quantitative PCR (Q-PCR) assay using SYBR green master mix and the ABI7500 system. Primer sequences for each gene were designed using PrimerExpress software and are listed in Table 1. Amplicons generated from each primer pair was around 50–100 bp. Loading of each sample was normalized with ROX dye. All readings were normalized to the expression of GAPDH.

2.5. Immunoblotting, inhibitor assay and immunofluorescence staining

For growth factor time course, PC12 cells were incubated in serum-free media containing 1% bovine serum albumin (BSA) overnight and treated with 100 ng/ml NGF or 100 ng/ml FGF1 and 10 μg/ml heparin for the time indicated. Cells were harvested into either RIPA (50 mM Tris, pH 7.5, 1% Triton X-100, 150 mM NaCl, 2 mM EGTA) (for STAT3 Western blotting) or L-RIPA buffer (50 mM Tris, pH 7.5, 0.1% Triton X-100, 150 mM NaCl, 2 mM EGTA) containing 1 mM Na_3VO_4, 1 mM phenylmethanesulphonylfluoride (PMSF), 10 ng/ml aprotinin and 10 ng/ml leupeptin. Protein concentration of each sample was

Table 1
Sequences of the Q-PCR primers used in this study.

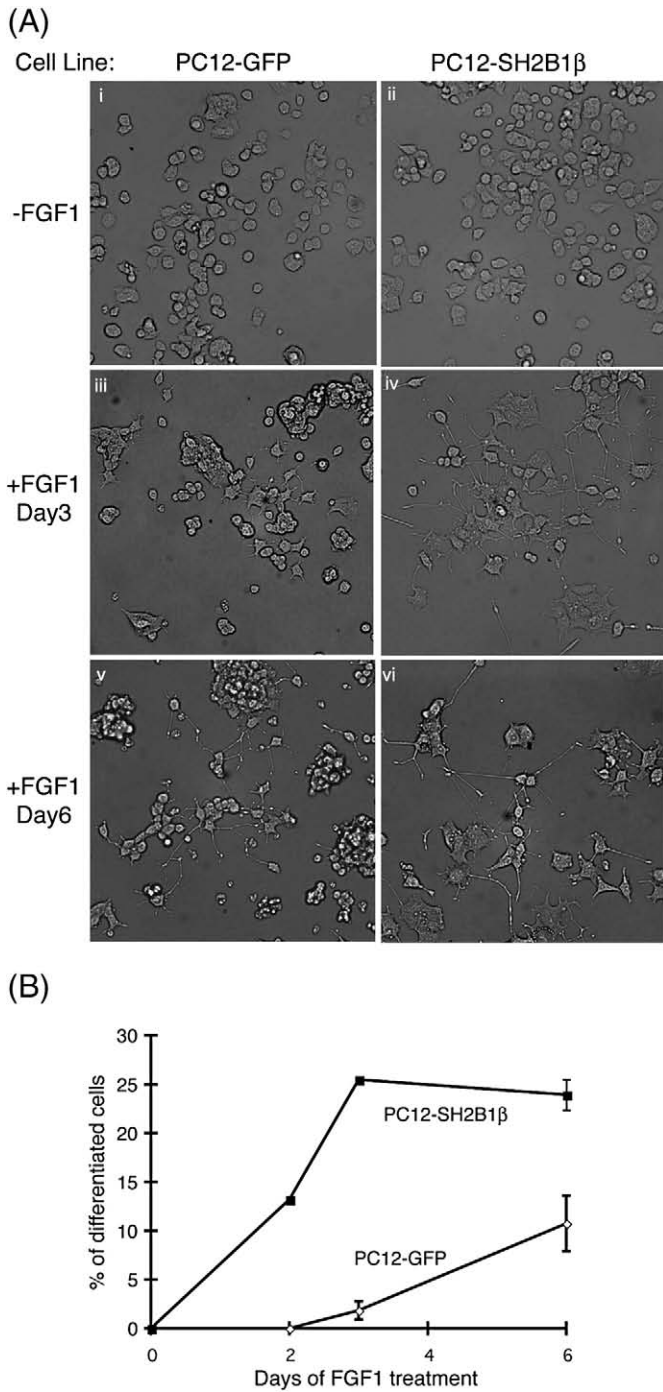| Gene	Sequence (5′ to 3′)
Egr1	
Forward	CAGTGGCCTTGTGAGCATGA
Reverse	GCAGAGGAAGACGATGAAGCA
p35	
Forward	ACAGCAAGAACGCCAAGGA
Reverse	TTCCAAGGCAGTACCGAGATG
GAPDH	
Forward	ATGACTCTACCCACGGCAAGTT
Reverse	TCCCATTCTCAGCCTTGACTGT

(A)

Fig. 1. Neurite outgrowth in PC12 cells overexpressing GFP (PC12-GFP) or GFP-SH2B1β (PC12-SH2B1β) in response to FGF1. (A) PC12-GFP cells (i, iii, v) and PC12-SH2B1β cells (ii, iv, vi) were treated with 100 ng/ml FGF1 plus 10 μg/ml heparin in low serum medium as described in Materials and methods section for 0 (i, ii), 3 (iii, iv) or 6 (v, vi) days. Representative images of live cells were shown. (B) The percentage of differentiated cells in PC12-GFP or PC12-SH2B1β cells was counted from 2 to 6 day after FGF1 treatment. Values were means ± standard deviation from two independent experiments. For each experiment, 300–400 cells were counted.

determined. Equal amount of proteins was loaded to and resolved by sodium dodecyl sulfate-polyacrylamide gel electrophoresis (SDS-PAGE) and then transferred to nitrocellulose paper for western blot analysis using the indicated antibodies. The immunoblots were detected using either Alexa Fluor 680-conjugated IgG and an Odyssey Infrared Imaging System (LI-COR Biosciences, Lincoln, NE) or horse-radish peroxidase-conjugated IgG and the ECL system. For inhibitor assays, PC12 cells were seeded about 80–85% confluency on 3.5 cm

dishes. PC12 cells were grown in serum-free medium containing 1% BSA for overnight and then pre-treated with or without the indicated inhibitor 1 h before adding 100 ng/ml FGF1 and 10 μg/ml heparin. At the indicated time points, cells were collected and lysed. The lysate was then analyzed via Western blotting. For immunofluorescence
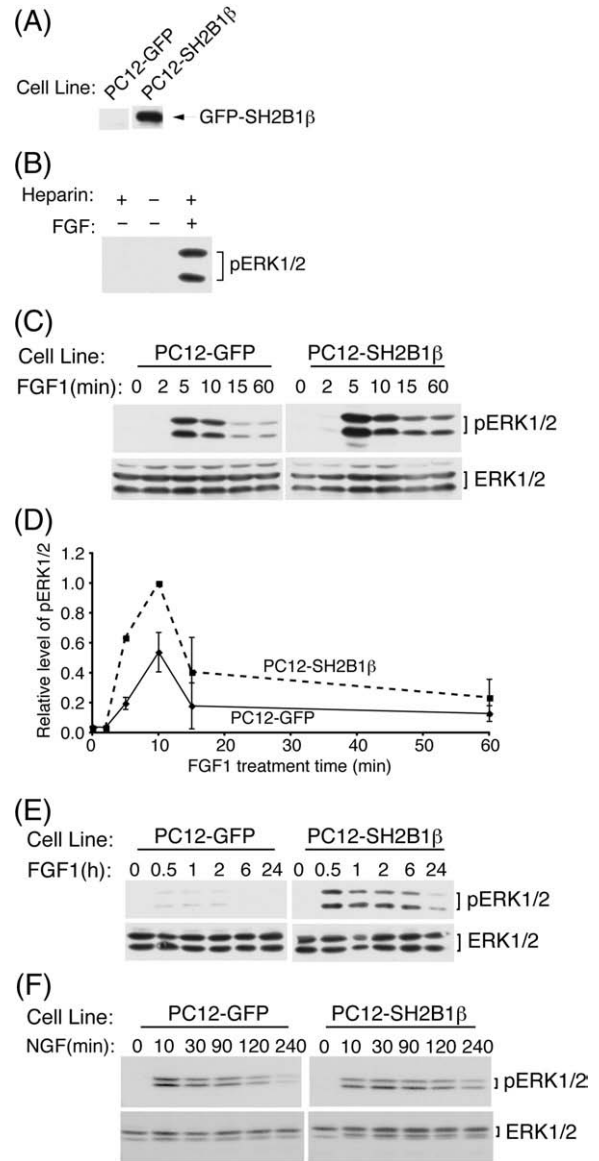

Fig. 2. The phosphorylation level of ERK1/2 in PC12-GFP and PC12-SH2B1β cells after FGF1 or NGF treatment. (A) Equal amount of proteins from lysates of PC12-GFP cells or PC12-SH2B1β cells was analyzed via SDS-PAGE and immunoblotted with anti-SH2B1β antibody to determine the expression of GFP-SH2B1β. (B) PC12-SH2B1β cells were incubated in serum-free medium overnight before stimulated with 10 μg/ml heparin only (lane 1), mock-treated (lane 2) or treated with 100 ng/ml FGF1 plus 10 μg/ml heparin (lane 3) for 5 min. Equal amount of proteins from the collected lysates was separated by SDS-PAGE and immunoblotted with anti-pERK1/2 antibody. (C) PC12-GFP or PC12-SH2B1β cells were in serum-free medium overnight before stimulation with 100 ng/ml FGF1 and 10 μg/ml heparin for the indicated time points. Lysates were collected and equal amount of proteins was separated by SDS-PAGE and immunoblotted with either anti-pERK1/2 or anti-ERK1/2 antibody. Representative blots from three independent experiments were shown. (D) pERK1/2 level was normalized to total ERK1/2 and the relative pERK1/2 level for the 10 min time point of PC12-GFPSH2B1β cells was used as 1.0. The error bars represent standard deviation from two independent experiments. (E) PC12-GFP or PC12-SH2B1β cells were treated as described in (C) for the indicated time points. Lysates were collected and equal amount of proteins was separated by SDS-PAGE and immunoblotted with either anti-pERK1/2 or anti-ERK1/2 antibody. (F) PC12-GFP or PC12-SH2B1β cells were stimulated by 100 ng/ml NGF for the indicated time points. Equal amount of proteins from the lysates was separated by SDS-PAGE and immunoblotted with either anti-pERK1/2 or anti-ERK1/2 antibody.
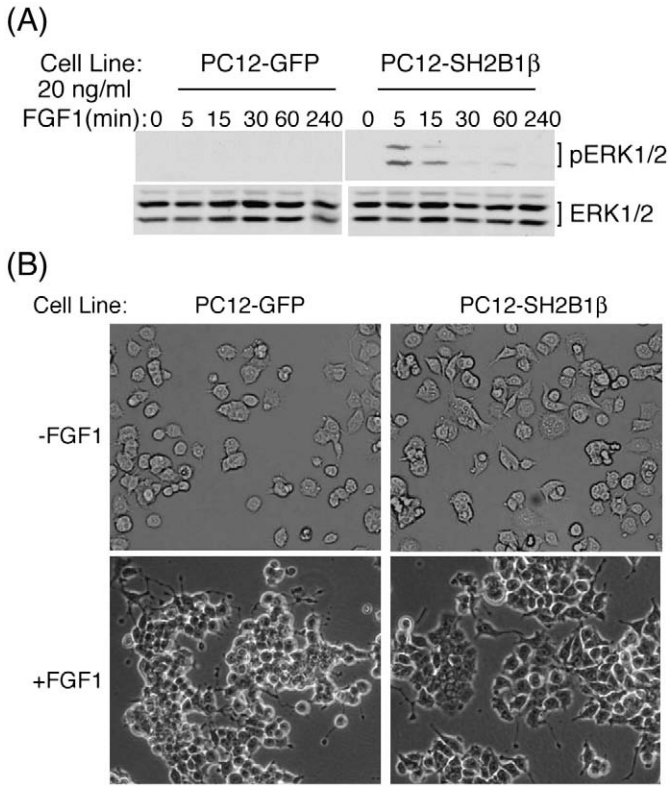
(A)

(B)

Fig. 3. The effect of low dosage of FGF1 on the phosphorylation of ERK1/2 and neurite outgrowth in PC12-GFP and PC12-SH2B1β cells. (A) PC12-GFP or PC12-SH2B1β cells were incubated in serum-free medium overnight before stimulation with 20 ng/ml FGF1 plus 2 μg/ml heparin for the indicated time points. Equal amount of proteins from the lysates was resolved by SDS-PAGE and immunoblotted with either anti-pERK1/2 or anti-ERK1/2 antibody. (B) PC12-GFP or PC12-SH2B1β cells were treated with 20 ng/ml FGF1 plus 2 μg/ml heparin in low serum medium as described in Materials and methods section. Neurite outgrowth was monitored and the representative images of live cells were taken after FGF1 treatment for 3days. Upper panels were taken with bright field while the lower panels were taken with phase contrast condition.

staining, PC12 cells were split onto 1:100 Matrigel-coated coverslip and treated as indicated. Cells were then fixed with 4% paraformaldehyde, permeabilized with 0.1% Triton X-100 followed by BSA blocking and antibody incubation. For neuronal tubulin immunostaining, monoclonal antibody to neuronal β-tubulin (TuJ1) was used at a dilution of 1:1000 followed by Alexa Fluor 594-conjugated anti-mouse IgG (1:1000) for visualization. Images were visualized and taken using the inverted Zeiss Axiover 135 fluorescence microscope.

3. Results

3.1. SH2B1β promotes FGF1-induced neurite outgrowth

FGF1 has previously been shown to induce neurite outgrowth in PC12 cells [50–52]. To determine the effect of SH2B1β in FGF1-mediated neurite outgrowth, we compared the neurite outgrowth between PC12 cells stably expressing GFP (PC12-GFP cell line) or GFP-SH2B1β (PC12-SH2B1β cell line). FGF1 needs heparin to elicit its physiological action, thus heparin was added together with FGF1 in all FGF1 treatment in this study unless otherwise noted. PC12-GFP and PC12-SH2B1β cell lines were treated with 100 ng/ml recombinant human FGF1 together with 10 μg/ml heparin for 0, 3 or 6 days in low serum-containing medium (as described in Materials and methods section). As in Fig. 1A, PC12-SH2B1β cells showed significantly higher percentage of neurite outgrowth and earlier initiation of neurite outgrowth (Fig. 1A, panels ii, iv and vi) compared with the control

PC12-GFP cells (Fig. 1, panels i, iii, and v). Fig. 1B shows the quantified result of FGF1-induced differentiation in PC12-GFP and PC12-SH2B1β cell lines. The definition of neuronal differentiation in PC12 cells is described in Materials and methods section. At all time points examined, PC12-SH2B1β cells had higher percentage of differentiated cells.

3.2. SH2B1β enhances and prolongs FGF1 signaling

To determine how SH2B1β promotes FGF1-induced neurite outgrowth, we compared the signaling pathways initiated by FGF1 in
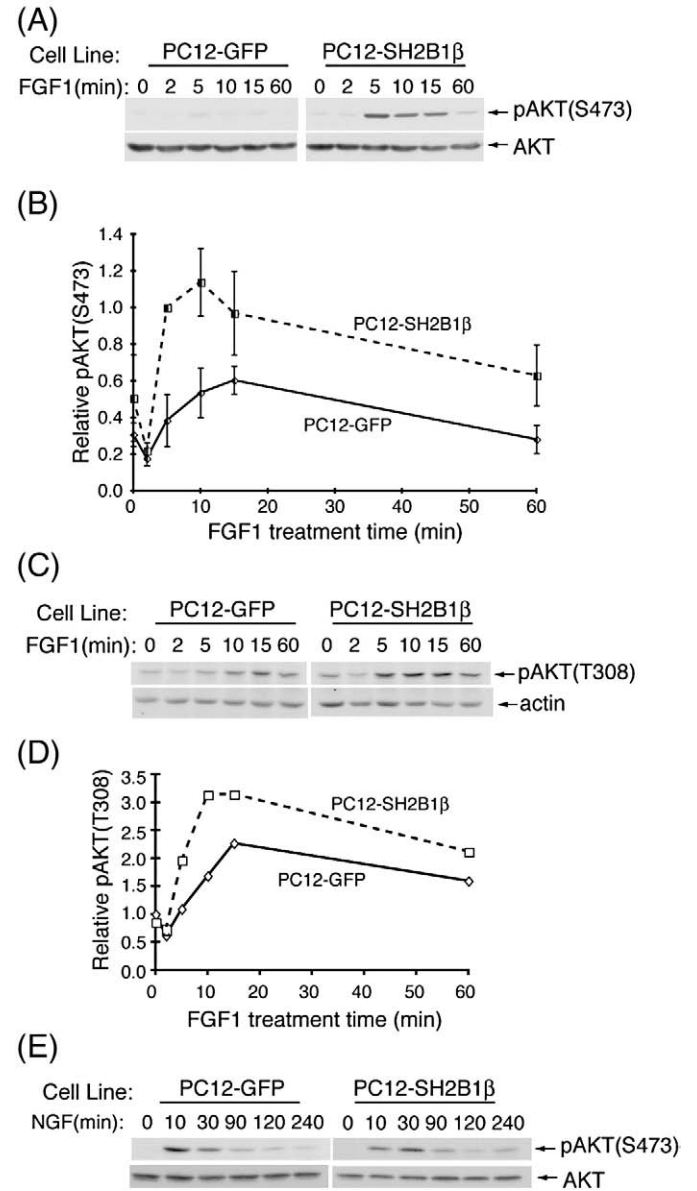
(A)

(B)

(C)

(D)

(E)

Fig. 4. The phosphorylation level of AKT in PC12-GFP and PC12-SH2B1β cells after FGF1 or NGF treatment. PC12-GFP or PC12-SH2B1β cells were incubated in no serum-containing medium overnight and then stimulated with (A, C) 100 ng/ml FGF1 plus 10 μg/ml heparin or (E) 100 ng/ml NGF for the indicated time. (A) Representative blots from three independent experiments were shown. Equal amount of proteins from the lysates was separated by SDS-PAGE and immunoblotted with either anti-pAKT(S473) or anti-AKT antibody (loading control). (B) Relative pAKT level was normalized to total AKT and the relative pAKT level for the 5 min time point of PC12-SH2B1β was used as 1. The error bars are standard errors from three independent experiments. (C) Equal amount of proteins from the lysates was separated by SDS-PAGE and immunoblotted with either anti-pAKT(T308) or anti-actin antibody (loading control). (D) Quantified results from (C) are shown using mock-treated control in PC12-GFP cells as 1.
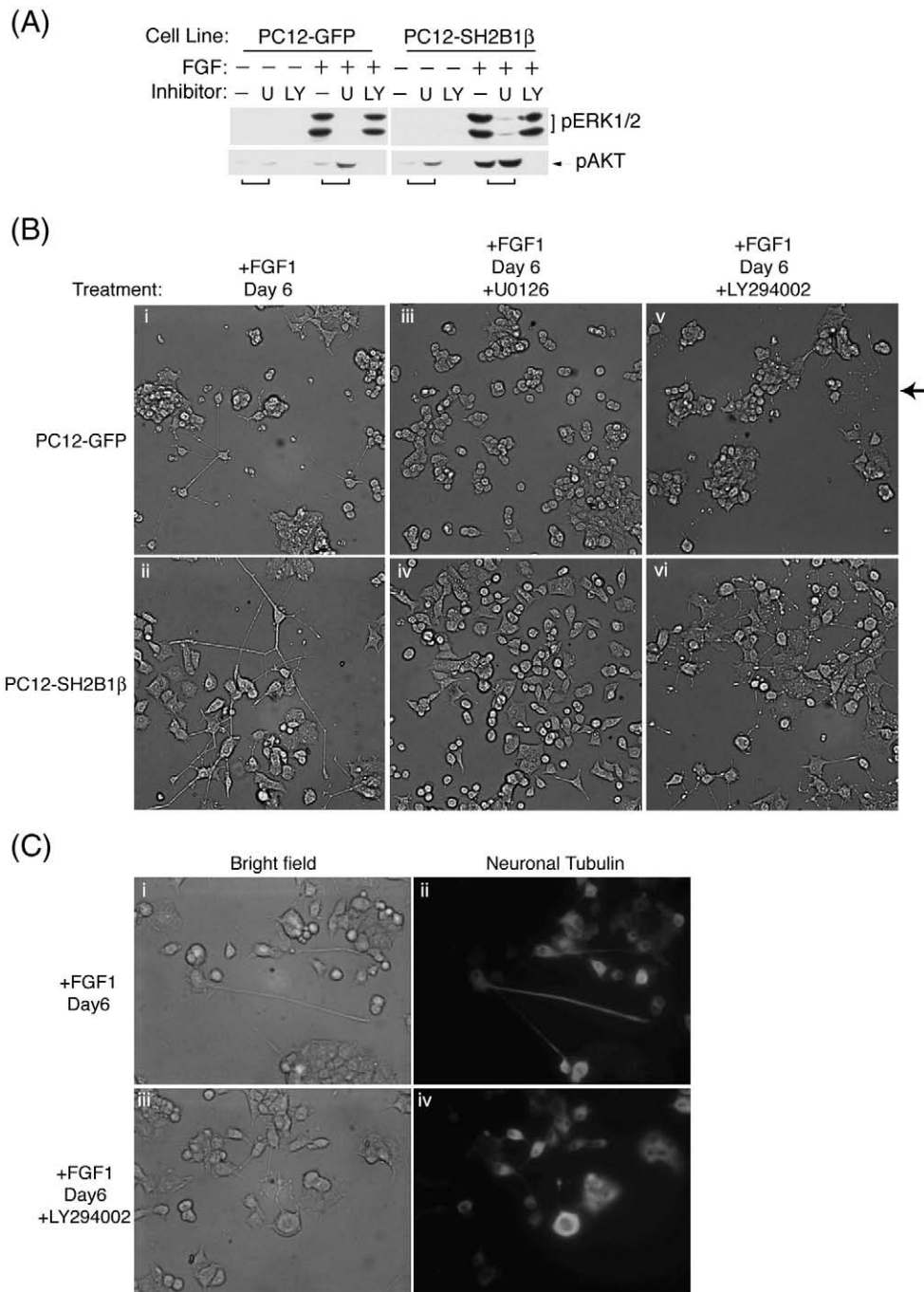
Fig. 5. Effect of U0126 and LY294002 on FGF1 signaling and FGF1-induced neurite outgrowth in PC12-GFP and PC12-SH2B1β cells. (A) PC12-GFP or PC12-SH2B1β cells were incubated in serum-free medium overnight and U0126 (20 μM) or LY294002 (20 μM) was added to cells 1 h before 10 min stimulation of 100 ng/ml FGF1. Equal amount of proteins from the lysate was resolved with SDS-PAGE and immunoblotted with anti-pERK1/2 or anti-pAKT(S473) antibody. The brackets indicate the increased pAKT in the presence of U0126 inhibitor. Representative blots from two independent experiments were shown. (B) PC12-GFP cells (panels i, iii and v) or PC12-SH2B1β cells (panels ii, iv and vi) were pre-treated with U0126 (20 μM) (panels iii and iv) or LY294002 (20 μM) (panels v and vi) for 1 h, followed by FGF1 stimulation in low serum medium. The neurite outgrowth was monitored for 6 days. Representative images of live cells were shown. Arrow points to the aberrant neurite morphology. (C) PC12-GFP (panels i and ii) or PC12-SH2B1β cells (panels iii and iv) were pre-treated with LY294002 as described in (B) followed by FGF1 stimulation for 6 days. Cells were then fixed for immunofluorescence staining with anti-TuJ1 and anti-mouse Alexa Fluor 594. Images were taken using Zeiss Axiovert 135 fluorescence microscopy.

PC12-GFP and PC12-SH2B1β cell lines. Fig. 2A shows that GFP-SH2B1β is overexpressed in PC12-SH2B1β cell line but not in PC12-GFP cells. To exclude the possibility that heparin would have effect on signaling, cells were mock-treated, treated with 10 μg/ml heparin alone or 100 ng/ml FGF1 plus 10 μg/ml heparin. The phosphorylation of ERK1/2 (pERK1/2) was determined via immunoblotting with anti-pERK1/2 antibody. As shown in Fig. 2B, heparin alone did not induce phosphorylation of ERK1/2 while FGF1 plus heparin induces pERK1/2. To determine the effect of SH2B1β on FGF1-induced signal transduction, both PC12-GFP and PC12-SH2B1β cell lines were treated with 100 ng/ml FGF1 in combination of 10 μg/ml heparin for the indicated time points. In the PC12-GFP cell line, pERK1/2 was detected 5 min after FGF1 stimulation, reduced by 15 min and the level of phosphorylation remains above the basal level for at least up to 60 min. In contrast, in

PC12-SH2B1β cell line, pERK1/2 was detected in 5 min of FGF1 treatment and the phosphorylation remained higher than that in PC12-GFP cells for at least 60 min (Fig. 2C). The magnitude of pERK1/2 in PC12-SH2B1β is increased compared with that in PC12-GFP cells. Total ERK1/2 immunoblot serves as the loading control to demonstrate that the difference of pERK1/2 in the two cell lines is not due to the difference in the total amount of ERK1/2 (Fig. 2C). The quantified result are shown in Fig. 2D. Prolonged pERK1/2 has been suggested to be an important determinant of neuronal differentiation. We thus examined the effect of FGF1 on the phosphorylation of ERK1/2 for up to 24 h. The pERK1/2 was detectable for at least 2 h in PC12-GFP cells and 24 h for PC12-SH2B1β (Fig. 2E). In contrast, the NGF-induced pERK1/2 is slightly more prolonged in PC12-SH2B1β cells compared to control cells while the degree of phosphorylation is not obviously increased in PC12-SH2B1β cells (Fig. 2F). These data suggest that SH2B1β significantly increases and prolongs FGF1-induced pERK1/2.

As the debate of whether activation of ERK1/2 is required for FGF1-induced neurite outgrowth continues [53], we tested the consequence of treating PC12 cells with lower dosage of FGF1 in phosphorylation of ERK1/2. As shown in Fig. 3A, pERK1/2 was not detectable in PC12-GFP cells when treated with 20 ng/ml FGF1. In contrast, this dosage of FGF1 was able to induce transient phosphorylation of ERK1/2 in PC12-SH2B1β cells, though to a much less degree compared with 100 ng/ml FGF1. The exposure time to obtain the pERK1/2 signal for Fig. 3A was approximately 15 times longer than in Fig. 2C. Nevertheless, this dosage was not able to induce morphological differentiation in either PC12-GFP or PC12-SH2B1β cells (Fig. 3B). Together, these data suggest that the phosphorylation of ERK1/2 needs to reach a "threshold" to initiate morphological differentiation of PC12 cells.

Similar to FGF1-induced pERK1/2, phosphorylation of AKT at Ser473 [pAKT(S473)] was detected 5 min after FGF1 stimulation and peaked at 15 min in PC12-GFP cells and 10 min in PC12-SH2B1β cells. The level of pAKT(S473) was increased and prolonged in PC12-SH2B1β compared with PC12-GFP cells (Fig. 4A). Quantified results are shown in Fig. 4B. SH2B1β also enhances FGF1-induced phosphorylation of AKT at Thr308 [pAKT(T308)] as shown in Fig. 4C and D. The patterns of FGF1-induced pAKT(S473) and pAKT(T308) are similar in the two cell lines. In response to NGF, on the other hand, pAKT(S473) was slightly more prolonged in PC12-SH2B1β cells than in PC12-GFP cells but the degree of phosphorylation was similar in both cell lines (Fig. 4E).

3.3. Phosphorylation of ERK1/2 is required for FGF1-induced neurite outgrowth

To delineate the contribution of MEK-ERK1/2 and PI3K-AKT pathway in FGF1-induced neurite outgrowth, we assessed the effect of blocking either of these two pathways. PC12-SH2B1β cells were pre-treated with either MEK or PI3K inhibitor 1 h before adding FGF1 or mock-treated for the indicated time and the neurite outgrowth was examined. The MEK inhibitor, U0126, inhibits FGF1-induced pERK1/2 without blocking pAKT signal in both cell lines (Fig. 5A, upper panel). PI3K inhibitor, on the other hand, blocks FGF1-induced pAKT(S473) (Fig. 5A, lower panel). Interestingly, we found that as pEKR1/2 being inhibited by MEK inhibitor, pAKT (S473) was increased (Fig. 5A, brackets). Using similar approach, we assessed the effect of these two inhibitors on FGF1-induced neurite outgrowth. No neurite outgrowth was found in U0126-treated cells (Fig. 5B, panels iii and iv) compared with mock-treated cells (Fig. 5B, panels i and ii). Interestingly, we found that LY294002-treated cells bear shorter neurites in response to FGF1 but the neurite outgrowth was not blocked (Fig. 5B, panels v and vi). In addition, LY294002-treated cells generated thinner neurites (panel v, arrow) than mock-treated cells. Immunostaining of the neuronal tubulin showed obvious expression of neuronal beta III tubulin in the neurites of FGF1-treated PC12-SH2B1β cells (Fig. 5C, panel ii) and

minimal expression in the neurites of LY294002-treated cells (Fig. 5C, panel iv). This finding suggests a possible role of PI3K-pAKT in neuronal tubulin expression/localization/stability in the neurites. Together, these results suggest that MEK-ERK1/2 pathway is required for FGF1-induced neurite outgrowth while PI3K-AKT pathway may serve to maintain neuronal phenotype and/or promote cell survival during neuronal differentiation.
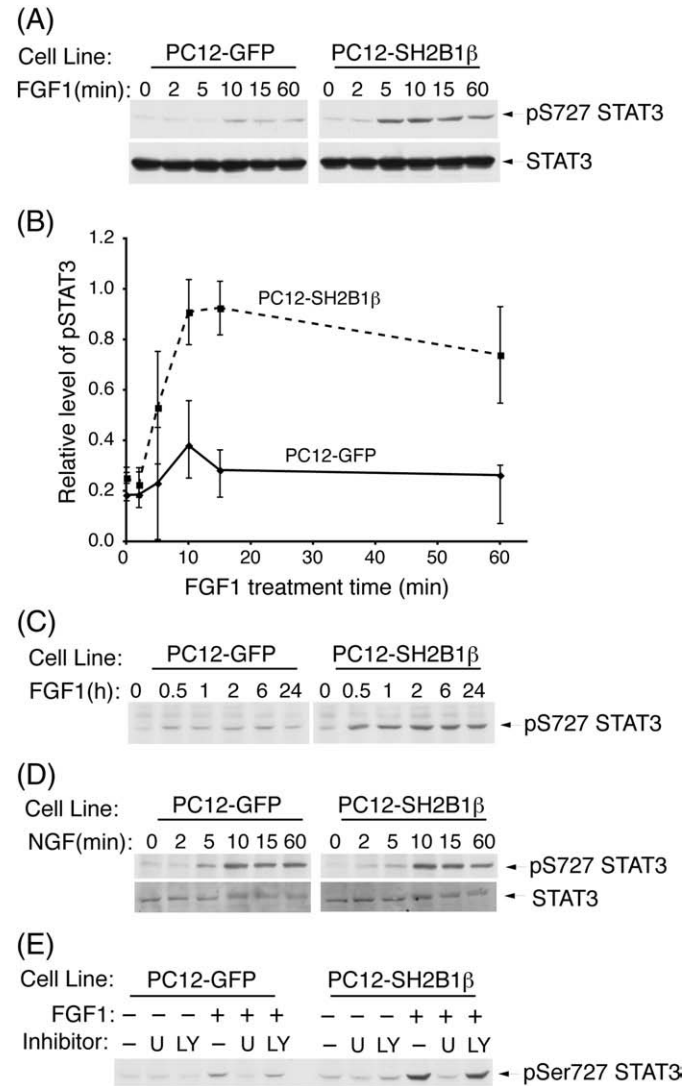

Fig. 6. SH2B1β enhances the FGF1-induced pSTAT3(S727) through MEK-ERK pathway. (A) PC12-GFP or PC12-SH2B1β cells were incubated in serum-free medium overnight before the addition of 100 ng/ml FGF1 and 10 μg/ml heparin for the indicated time points. Equal amount of proteins from the lysates was loaded, resolved with SDS-PAGE and immunoblotted with anti-pSTAT3(S727) or anti-STAT3 antibody. Representative blots from three independent experiments were shown. (B) Relative pSTAT3 was normalized to total STAT3 level. The highest relative pSTAT3 level in each experiment was regarded as 1.0. The error bars represent standard deviation from two independent experiments. (C) PC12-GFP or PC12-SH2B1β cells were incubated in serum-free medium overnight before 100 ng/ml FGF1 treatment for the indicated time points. Equal amount of proteins from each lysate sample was analyzed with SDS-PAGE and immunoblotted with anti-pSTAT3(S727) antibody. (D) PC12-GFP or PC12-SH2B1β cells were incubated in serum-free medium overnight before the addition of 100 ng/ml NGF for the indicated time points. Equal amount of proteins from the lysates was loaded, resolved with SDS-PAGE and immunoblotted with anti-pSTAT3(S727) or anti-STAT3 antibody. (E) Cells were incubated in serum-free medium for 8 h, then U0126 (20 μM) or LY294002 (20 μM) was added to cells 1 h before 100 ng/ml FGF1 and 10 μg/ml heparin stimulation for 10 min. Cell lysate was collected and equal amount of proteins was analyzed with SDS-PAGE and immunoblotted with anti-pSTAT3(S727) antibody.

3.4. FGF1-induced STAT3 phosphorylation is through MEK-ERK1/2 pathway

To delineate the downstream event of MEK-ERK1/2 pathway, we examined the effect of FGF1 on a candidate transcription factor, signal transducer and activator of transcription 3 (STAT3). The serine phosphorylation of STAT3 has been reported to be a downstream effector of NGF signaling in PC12 cells recently [54]. However, this phosphorylation had not been shown for FGF1 signaling in PC12 cells. To determine whether STAT3 is phosphorylated by FGF1, PC12-GFP and PC12-SH2B1β cells were challenged with FGF1 for the indicated time points and cell lysates from PC12-GFP or PC12-SH2B1β were assayed for the serine 727 phosphorylation of STAT3 [pSTAT3(S727)]. Our data showed that FGF1 induced pSTAT3(S727) in both cell lines (Fig. 6A). The induced pSTAT3(S727) was detected 10 min after FGF1 treatment in PC12-GFP cells and as early as 5 min of FGF1 stimulation in PC12-SH2B1β cells (Fig. 6A, upper panel). The level of total STAT3 among all samples was similar demonstrating that the difference of pSTAT3(S727) was not due to loading difference (Fig. 6A, bottom panel). The quantified results are shown in Fig. 6B. The FGF1-induced pSTAT3(S727) prolonged till at least 24 h in response to FGF1 (Fig. 6C). This is the first evidence demonstrating that FGF1 induces the

phosphorylation of STAT3 at S727 in PC12 cells and that overexpressing SH2B1β allows earlier phosphorylation as well as prolongs the phosphorylation. In contrast, SH2B1β did not enhance NGF-induced pSTAT3(S727) nor prolong it (Fig. 6D).

Our new finding that pSTAT3(S727) was induced by FGF1 prompts us to ask which pathway leads to this phosphorylation. Prospective candidates are serine/threonine kinases in the ERK1/2 and AKT pathways. Thus, using the specific inhibitors of MEK and PI3K, we assessed their effect on pSTAT3(S727). As shown in Fig. 6E, inhibiting MEK by U0126 blocked phosphorylation of FGF1-inducecd pSTAT3 (S727) in both PC12-GFP and PC12-SH2B1β cell lines. In contrast, inhibiting AKT phosphorylation by LY294002 did not affect pSTAT3 (S727). This data suggest, for the first time, that MEK-ERK1/2 pathway is responsible for the FGF1-induced pSTAT3(S727) in PC12 cells.

3.5. SH2B1β enhances and prolongs FGF1-induced Egr1 expression

Our results using U0126 inhibitor have suggested that MEK-ERK1/2 pathway is required for FGF1-induced neurite outgrowth (Fig. 5). To further delineate the downstream events of this pathway, we have examined the expression, both at mRNA and protein levels, of the immediate early gene — Egr1. As shown in Fig. 7A, the mRNA level of
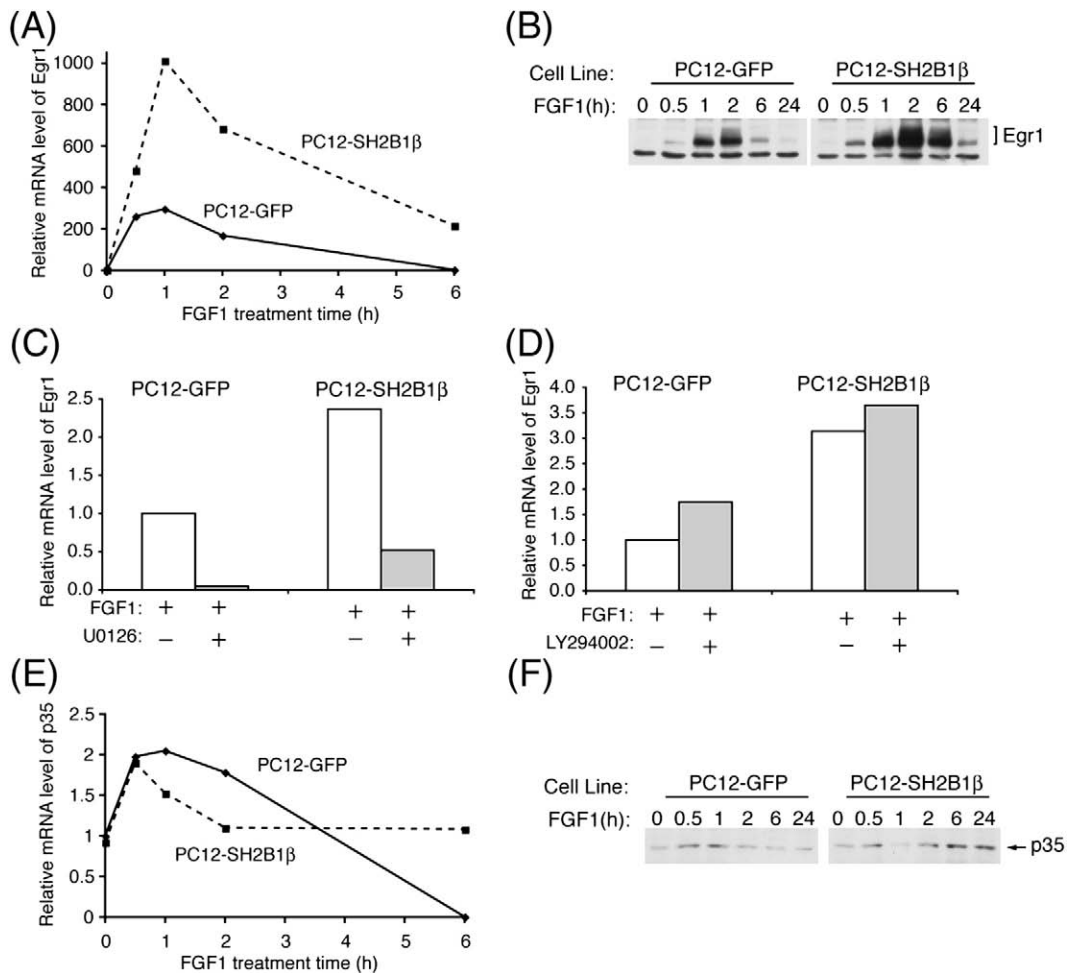

Fig. 7. SH2B1β enhances FGF1-induced expression level of Egr1 without significant effect on the expression level of p35. (A) PC12-GFP or PC12-SH2B1β cells were incubated in serum-free medium overnight and then treated with 100 ng/ml FGF1 and 10 μg/ml heparin for the indicated time points. Total RNAs were extracted and convert to cDNA and expression level of Egr1 was quantified by Q-PCR. The relative expression level of Egr1 was normalized with the expression of the housekeeping gene, GAPDH. (B) Cells were treated as described in (A). Equal amount of proteins from lysates was resolved by SDS-PAGE and the level of Egr1 was determined via Western blotting using anti-Egr1 antibody. (C, D) Cells were treated as described in (A) except the pretreatment of 20 μM U0126 (C) or 20 μM LY294002 (D) 1 h before FGF1 induction for another hour. Egr1 expression level was quantified by Q-PCR as described in (A). (E) Cells were treated as described in (A). RNAs were collected for the subsequent Q-PCR analysis to determine the expression level of p35. Expression level of p35 was normalized with GAPDH. (F) Cells were treated as described in (A). Equal amount of proteins from lysates was resolved by SDS-PAGE and the level of p35 was determined via Western blotting using anti-p35 antibody.

Egr1 was induced as early as 30 min after FGF1 treatment for more than 200 fold. Its level peaked at 1 h and declined afterwards. This expression time course is similar in both cell lines while the expression level is higher and more prolonged in PC12-SH2B1β cells. The same expression pattern holds true for the Egr1 protein level. The FGF1-induced Egr1 protein expression was detectable 30 min after FGF1 stimulation and peaked at 2 h for both cell lines. The expression of Egr1 is dramatically higher in PC12-SH2B1β cells compared with PC12-GFP cells at all time points tested. At 1 h time point, Egr1 expression in PC12-SH2B1β cells was at least 3 times higher than that in PC12-GFP cells. Egr1 remained detectable even 24 h after FGF1 treatment in PC12-SH2B1β cells (Fig. 7B). To determine which pathway leads to induction of Egr1 expression, cells were pretreated with U0126 or LY294002 for 1 h before FGF1 induction for another hour. The expression level of Egr1 was determined using real time quantitative PCR (Q-PCR). The FGF1-induced Egr1 level in PC12-SH2B1β cells is approximately 2.5 fold of that in PC12-GFP cells and is dramatically reduced by the treatment of MEK inhibitor (Fig. 7C) and not affected by PI3K inhibitor (Fig. 7D), suggesting that FGF1-induced Egr1 expression is predominantly through MEK-ERK1/2 pathway. p35, a candidate target gene of Egr1, is the regulatory sub-unit of Cdk5. Upon binding to Cdk5, p35 increases the kinase activity of Cdk5/p35 complex to promote neurite outgrowth [55,56]. Because the promoter region of p35 contains an Egr1 binding site, we examined whether FGF1 would induce the expression of p35 and whether SH2B1β would have a role in p35 expression. In PC12-GFP cells, the FGF1-induced mRNA level of p35 was twice of the basal level, peaked at 1 h and declined to lower than the basal level by 6 h. In PC12-SH2B1β cells, p35 level peaked at 30 min, declined afterwards to near basal level for at least 6 h after FGF1 treatment (Fig. 7E). The protein expression pattern of p35 mirrors the mRNA level in that it peaked around 30 min to 1 h after FGF1 stimulation. The level declined after 1 h of FGF1 treatment in PC12-GFP cells while prolonged in PC12-SH2B1β cells (Fig. 7F). Over-expression of SH2B1β did not result in significant increase of p35. Because the degree of up-regulation of FGF1-induced Egr1 is much more dramatic than that for p35, FGF1-induced Egr1 expression does not likely to result in induction of p35.

3.6. Structural domains that mediate SH2B1β's enhancement of FGF1-induced neurite outgrowth

SH2B1β contains proline-rich, PH, and SH2 domains. To determine which domains are responsible for SH2B1β-mediated enhancement of FGF1-induced neurite outgrowth, we assessed the FGF1-induced neuronal differentiation among stable cell lines that express various mutation constructs of SH2B1β. The domain structures of SH2B1β mutants are depicted in Fig. 8A. SH2B1β(270–670) lacks the N-terminal proline-rich domains, SH2B1β(397–670) has no N-terminal proline-rich and PH domain, and SH2B1β(R555E) is the dominant negative mutant with a point mutation at the FLVR motif within the SH2 domain. When these cell lines were treated with FGF1 for the indicated time period, PC12-SH2B1β cells showed the highest enhancement on neuronal differentiation, followed by PC12-SH2B1β(270–670) and PC12-SH2B1β(397–670) cells, and the differentiation percentage in PC12-SH2B1β(R555E) cells was lower than that in PC12-GFP cells (Fig. 8B). Removing N-terminal proline-rich regions significantly reduced SH2B1's ability to enhance FGF1-induced neurite outgrowth suggesting that proteins binding to these regions may contribute to the positive effect of SH2B1β in neurite outgrowth. Interestingly, we found that PC12-SH2B1β(270–670) cells initiated neurites faster than PC12-SH2B1β(397–670) cells while the percentage of differentiation of PC12-SH2B1β(397–670) cells was higher than PC12-SH2B1β(270–670) after 3 days of FGF1 treatment. With a point mutation within the SH2 domain, the dominant negative mutant, SH2B1β(R555E), inhibited the ability of SH2B1β to enhance neurite outgrowth.

Our earlier results suggest that SH2B1β enhances FGF1-induced neurite outgrowth through MEK-ERK1/2 pathway. We thus determine the effect of SH2B1β truncation mutants in FGF1-induced pERK1/2. As demonstrated in Fig. 9A, PC12-SH2B1β showed enhanced FGF-induced pERK1/2 compared with the control PC12-GFP cells. PC12-SH2B1β(R555E) showed similar level of FGF1-induced pERK1/2 with control cells. This result is consistent with previously reported result that SH2B1β(R555E) did not inhibit NGF-induced neurite outgrowth
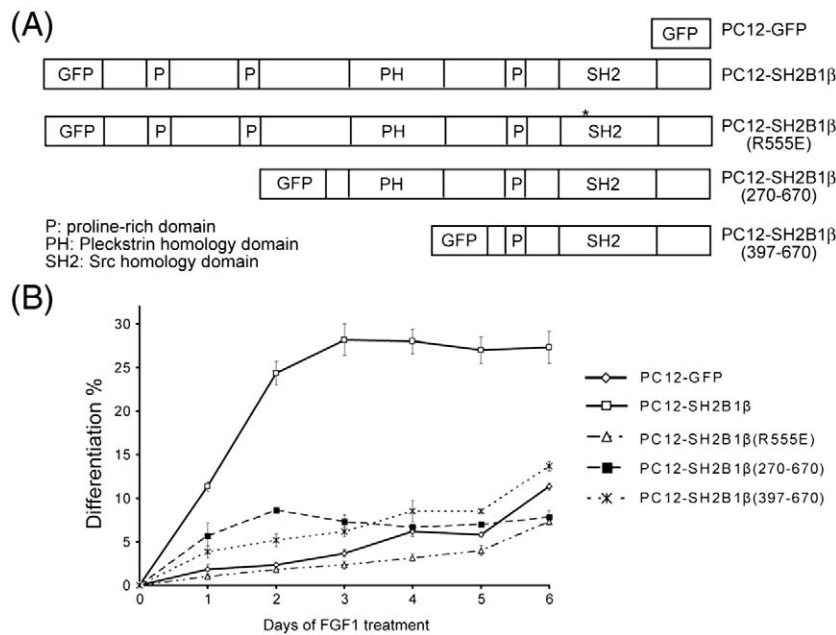

Fig. 8. Proline-rich, PH and SH2 domains of SH2B1β are required for its ability to enhance FGF1-induced neurite outgrowth. (A) Domain structures in various SH2B1β constructs are shown. (B) PC12 stable cell lines that express either of the constructs as in (A) were subjected to FGF1 treatment for 0 to 6 days. The percentage of neuronal differentiation was scored as described in the Materials and methods section. More than 200 cells were counted for each cell line per time point. Data are from 3 independent experiments and the error bars represent standard errors.
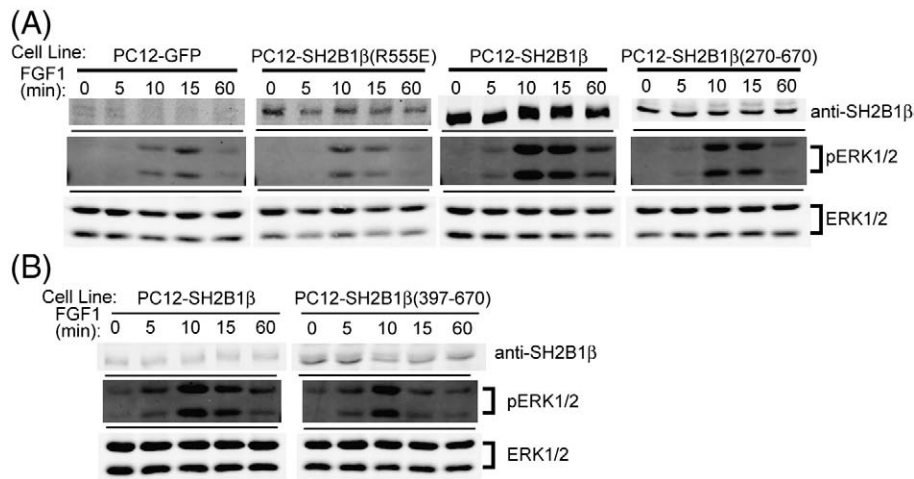
Fig. 9. The ability of SH2B1β mutants in promoting FGF1-induced neurite outgrowth corresponds to pERK1/2 level. PC12 cells stably expressing (A) GFP, GFP-SH2B1β(R555E), GFP-SH2B1β or GFP-SH2B1β(270–670), (B) GFP-SH2B1β or GFP-SH2B1β(397–670) were stimulated with 100 ng/ml FGF1 for the indicated time period and the induced level of pERK1/2 was determined via Western blotting. Total ERK11/2 was used as loading control.

through inhibiting NGF signaling [44]. PC12-SH2B1β(270–670) showed reduced pERK1/2 compared with PC12-SH2B1β cells but higher than the control cells. PC12-SH2B1β(397–670) also showed reduced pERK1/2 compared with PC12-SH2B1β cells (Fig. 9B). These results are consistent with our earlier conclusion that SH2B1β enhances FGF1-induced neurite outgrowth mainly through MEK-ERK1/2 pathway.

3.7. Inhibiting ROCK activity enhances FGF1-induced neurite outgrowth

It has previously been shown that ciliary neurotrophic factor (CNTF) rescued retinal ganglion cells (RGC) from axotomy-induced apoptosis through JAK-STAT3 pathway [57,58]. A recent study used JAK2 inhibitor, AG 490, to block the activation of STAT3 and showed that inhibiting CNTF-induced tyrosyl phosphorylation of STAT3 increased neurite outgrowth of RGC [59]. Furthermore, inhibiting Rho kinase (ROCK) activity using Y-27632 inhibited tyrosyl phosphorylation of STAT3 and increased neurite outgrowth. Our results indicate that SH2B1β enhances FGF1-induced neurite outgrowth through Ser727 phosphorylation of STAT3. We did not detect obvious induction of Tyr705 phosphorylation of STAT3 during FGF1 treatment (data not shown). Nonetheless, to examine whether ROCK activity would affect FGF1-induced neurite outgrowth and pSTAT3(S727), we treated PC12 cells without or with Y-27632 and monitored the neurite outgrowth. As demonstrated in Fig. 10A, compared with medium-only controls, treating PC12-GFP, PC12-SH2B1β, PC12-SH2B1β(R555E), PC12-SH2B1β(270–670) and PC12-SH2B1β(397–670) stable cell lines with Y-27632 induced neuronal sprouting (short neurites) but did not result in neuronal differentiation. Interestingly, inhibiting ROCK activity enhanced FGF1-induced neurite outgrowth in all stable cell lines tested on 3 or 6 days after FGF1 stimulation (Fig. 10B). To determine whether inhibiting ROCK activity affects FGF1-induced pSTAT3(S727), we treated all five stable cell lines with Y-27632, FGF1 or both and examined pSTAT3(S727) through Western blotting. Fig. 11A showed that in the presence of Y-27632, FGF1-induced pSTAT3(S727) was not reduced. This is true for all five stable cell lines. In fact, the extent of FGF1-induced pSTAT3(S727) correlated with their neurite outgrowth ability. Comparing with PC12-SH2B1β cells, PC12-SH2B1β(270–670) and PC12-SH2B1β(397–670) cells showed reduced pSTAT3(S727) in response to FGF1. Quantified results are shown in Fig. 11B. Consistent with what Lingor et al. has shown, we

also found that inhibiting ROCK increased induced level of pERK1/2 and pAKT(S473) level (Fig. 11C) [59].

Our current working model of how SH2B1β enhances FGF1-induced neurite outgrowth is depicted in Fig. 12. SH2B1β enhances FGF1-induced MEK-ERK1/2 and PI3K-AKT signaling pathways as well as increased pSTAT3(S727) resulting in the up-regulation of Egr1 expression. Inhibiting ROCK activity enhances FGF1-induced neurite outgrowth through pSTAT3(S727)-independent pathway.

Taken together, we have found that overexpressing the adaptor protein SH2B1β enhances FGF1-induced neurite outgrowth in PC12 cells. Our data demonstrate that SH2B1β enhances and prolongs the signaling initiated by FGF1, including the phosphorylation of ERK1/2 and AKT. A novel FGF1-induced signaling pathway that we have identified is the MEK-ERK1/2-STAT3 pathway. SH2B1β enhances and prolongs FGF1-induced pSTAT3(S727) as well as the expression of Egr1, which are MEK-ERK1/2-dependent.

4. Discussion

SH2B1β is a signaling adaptor protein, originally identified to interact with Janus kinase 2 (Jak2) and regulates growth hormone signaling [42]. Accumulating data add its significance through identifying its binding partner, such as FGFR3, TrkA, Ret, platelet-derived growth factor, insulin receptor, insulin growth factor 1 and tyrosine kinase Jak2, thus regulates their downstream signaling and physiological outcomes [41,42,44,49,60–62]. In this study, we presented evidence that PC12 cells stably expressing GFP-SH2B1β promote FGF1-induced neurite outgrowth. FGF1-induced phosphorylation of ERK1/2 and AKT was enhanced as well as prolonged in PC12-SH2B1β cells compared with control cells. Inhibiting pERK1/2 with MEK inhibitor blocks FGF1-induced neurite outgrowth and SH2B1β-mediated enhancement of neurite outgrowth strongly suggest the requirement of MEK-ERK1/2 in FGF1-induced neurite outgrowth. A study by Renaud et al. concluded that the neurotrophic activity of FGF1 is independent of ERK1/2 pathway [53]. To address the requirement of pERK1/2, we have examined pERK1/2 level with different dosages of FGF1. At 20 ng/ml FGF1, pERK1/2 was detected but no obvious morphological differentiation was observed after 3 days of treatment. One the other hand, 100 ng/ml FGF1 resulted in much higher pERK1/2 accompanied with morphological differentiation. Based on these results, we conclude that pERK1/2 needs to reach a threshold to initiate neurite outgrowth in PC12 cells. In addition,

prolonged pERK1/2 signal is required for neurite outgrowth. Low dosage of FGF1 only elicits transient pERK1/2 and is not sufficient to lead to neurite outgrowth. Therefore, the statement by Renaud et al. that "the neurotrophic activity of FGF1 is independent of ERK1/2 pathway" is not entirely correct. Interestingly, inhibiting pERK1/2 increased the level of pAKT (Fig. 5A), the expression of Egr1 (Fig. 7D) and number of cells bearing neurites (Fig. 5B and data not shown). This finding raises a possibility that MEK-ERK1/2 and PI3K-AKT pathways crosstalk to orchestrate the signal for FGF1-induced neurite outgrowth. To our surprise, blocking phosphorylation of AKT by LY294002 did not prevent FGF1-induced neurite outgrowth. Nevertheless, the neurites generated from LY294002-treated cells appeared thinner, indicative of being less healthy (Fig. 5B, panels v, vi). In addition, the expression of neuronal beta III tubulin in the LY294002-treated neurites was much reduced (Fig. 5C), suggesting that FGF1-induced pAKT may be involved in neuronal tubulin assembly or stability in the neurites and thus the maintenance of neuronal phenotype. Nonetheless, we cannot exclude the possibility that LY294002

would inhibit kinases other than AKT to modulate FGF1-induced neurite outgrowth and survival.

To further delineate the role of FGF1-dependent MEK-ERK1/2 activation, we have identified STAT3 transcription factor as one of the downstream effectors. The established paradigm of tyrosine phosphorylation of STATs is mediated through Janus kinase (JAK) family of receptor tyrosine kinases, cytokine receptors or growth factors [63–67]. S727 phosphorylation of STAT3 has just begun to gain its share of attention recently and is believed to confer maximal transcriptional activity of cytokines by recruiting p300 [68,69]. In this study, we have shown that pSTAT3(S727) was induced upon FGF1 stimulation and the induction is enhanced and prolonged by SH2B1β overexpression. Phosphorylation of S727 at STAT3 has been implicated in the postnatal rat brain development, during retinoid acid-induced neuronal differentiation of embryonic stem cells and during NGF treatment in PC12 cells [54,70,71]. Our data of FGF1 inducing pSTAT3(S727) corroborates these findings (Fig. 6). The induced pSTAT3(S727) was enhanced by overexpressing SH2B1β and was inhibited by MEK
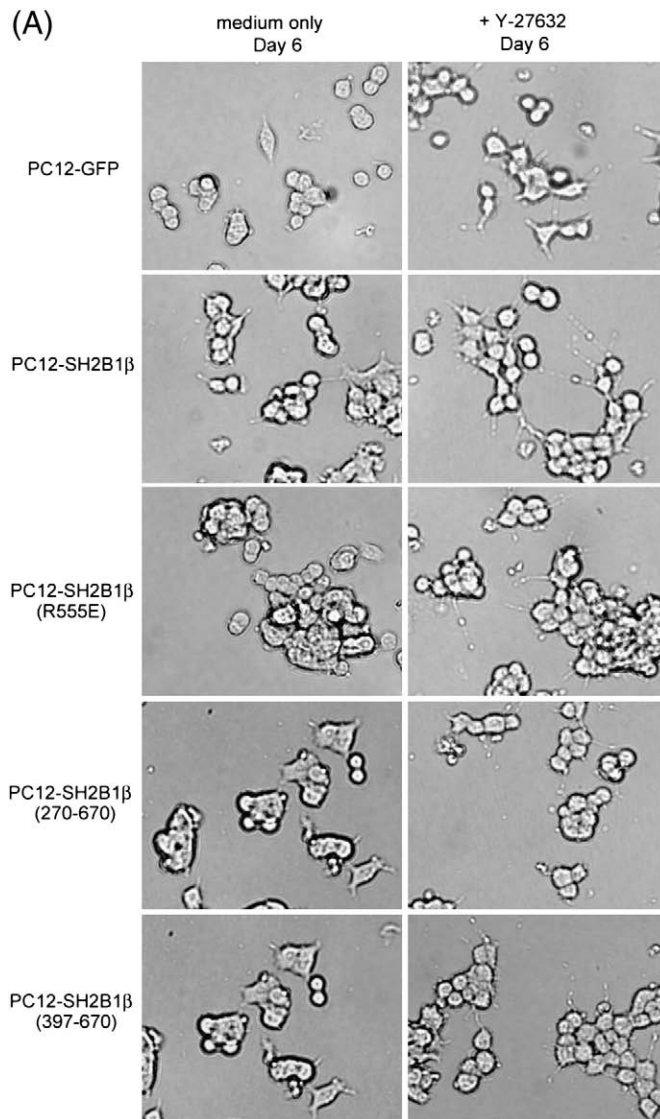

Fig. 10. Inhibiting ROCK enhances FGF1-induced neurite outgrowth. PC12 cells stably expressing GFP, GFP-SH2B1β, GFP-SH2B1β(R555E), GFP-SH2B1β(270–670) or GFP-SH2B1β(397–670) were incubated (A) in differentiation medium only or with 10 μM ROCK inhibitor, Y-27632, for 6 days; or (B) with 100 ng/ml FGF1 in the absence or presence of 10 μM Y-27632 for 3 or 6 days. Y-27632 was added 1 h before FGF1 addition. Bright field images of live cells from each indicated condition were taken using inverted Zeiss Axiover 135 fluorescence microscope. Representative images are shown.
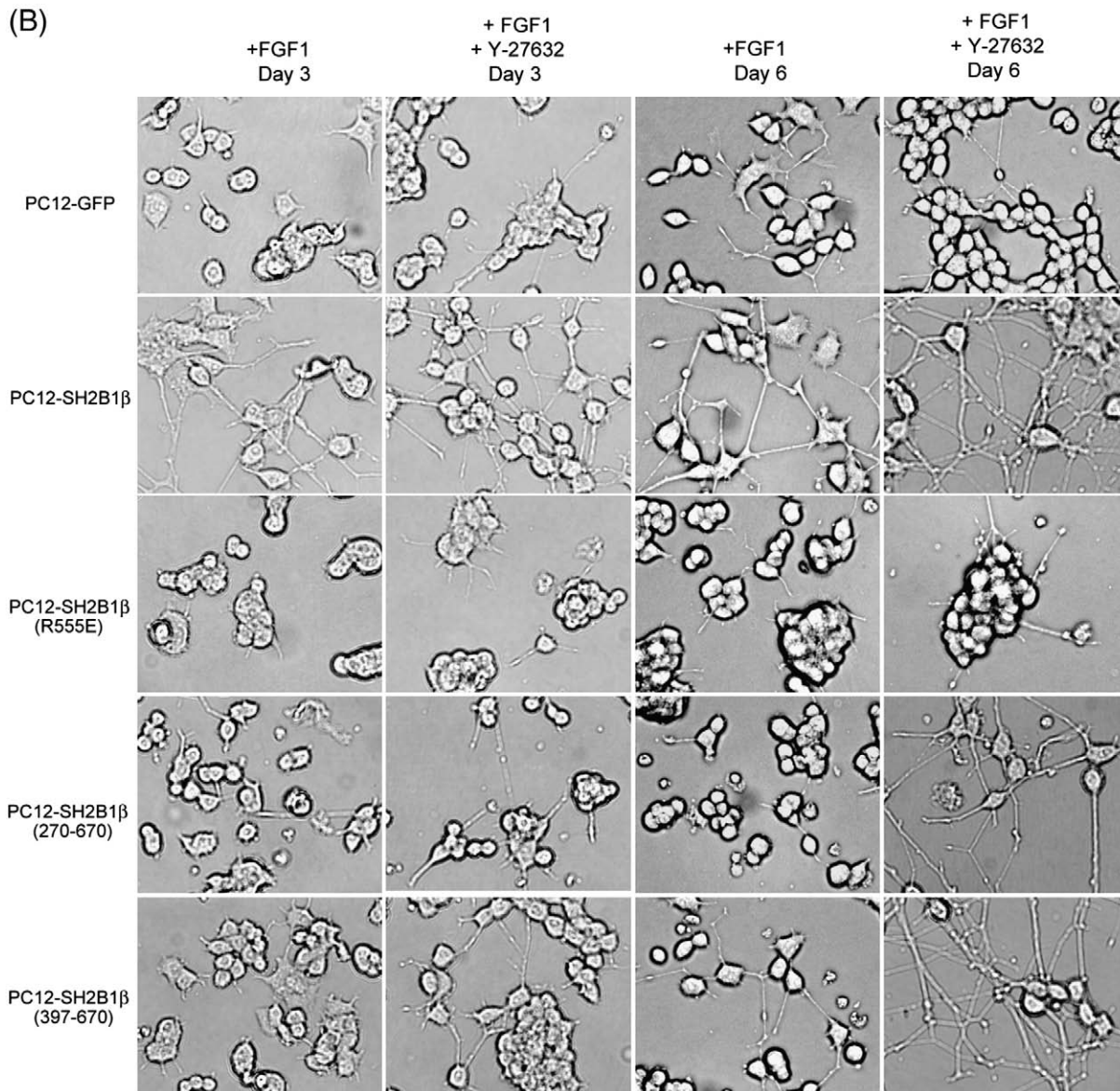
Fig. 10 (*continued*).

inhibitor suggesting that SH2B1β enhances MEK-ERK1/2 to increase pSTAT3(S727). This result presents the second STAT family member, in addition to STAT5, that is regulated by SH2B1β. In this study, we also showed that SH2B1β enhances FGF1-induced expression of immediate early gene, Egr1. Furthermore, we demonstrate that FGF1-induced Egr1 expression is through MEK-ERK1/2 pathway. Collectively, our data reveal the possibility that pSTAT3(S727) plays an essential role in mediating FGF1-induced signaling and gene expression required for neurite outgrowth.

Unlike NGF, FGF1-induced Egr1 does not result in increased expression of p35 despite the promoter region of p35 contains an Egr1 binding site. This result reveals a novel finding that NGF and FGF1 use distinct mechanisms to promote neurite outgrowth in PC12 cells. In addition, our results agree with previous findings that over-expression of SH2B1β does not increase NGF-induced pERK1/2 and pAKT [44]. The pattern of SH2B1β-regulated GDNF-induced signaling and neurite outgrowth mirrors its regulation on NGF-dependent signaling [44,49]. The differential regulation of SH2B1β on NGF and GDNF versus FGF1-induced signaling implies that SH2B1β utilizes different mechanisms to promote neurite outgrowth depending on the neurotrophic factors.

We further determined the domains within SH2B1β that are required for its ability to enhance FGF1-induced neurite outgrowth. With a point mutation in SH2 domain, SH2B1β(R555E) inhibited the ability of SH2B1β to promote neurite outgrowth but did not inhibit FGF1-induced pERK1/2. This finding is consistent with the previous result suggesting that SH2B1β(R555E) inhibited NGF-induced neurite outgrowth through mechanisms other than inhibiting NGF signaling [44]. Removing N-terminal proline-rich domains significantly reduced FGF1-initiated neurite outgrowth. With additional PH domain deleted, the neurite elongation catched up at later stage of differentiation. These results reveal a possibility that the proline-rich regions and the PH domain may have distinct roles in neurite initiation and elongation. Further studies shall cast insight on what SH2B1β-interacting proteins/protein complex are involved in SH2B1β-mediated neurite outgrowth.

Neuronal morphology is in part determined through the regulation of the cytoskeleton. Rho family of GTPase are key regulators of actin
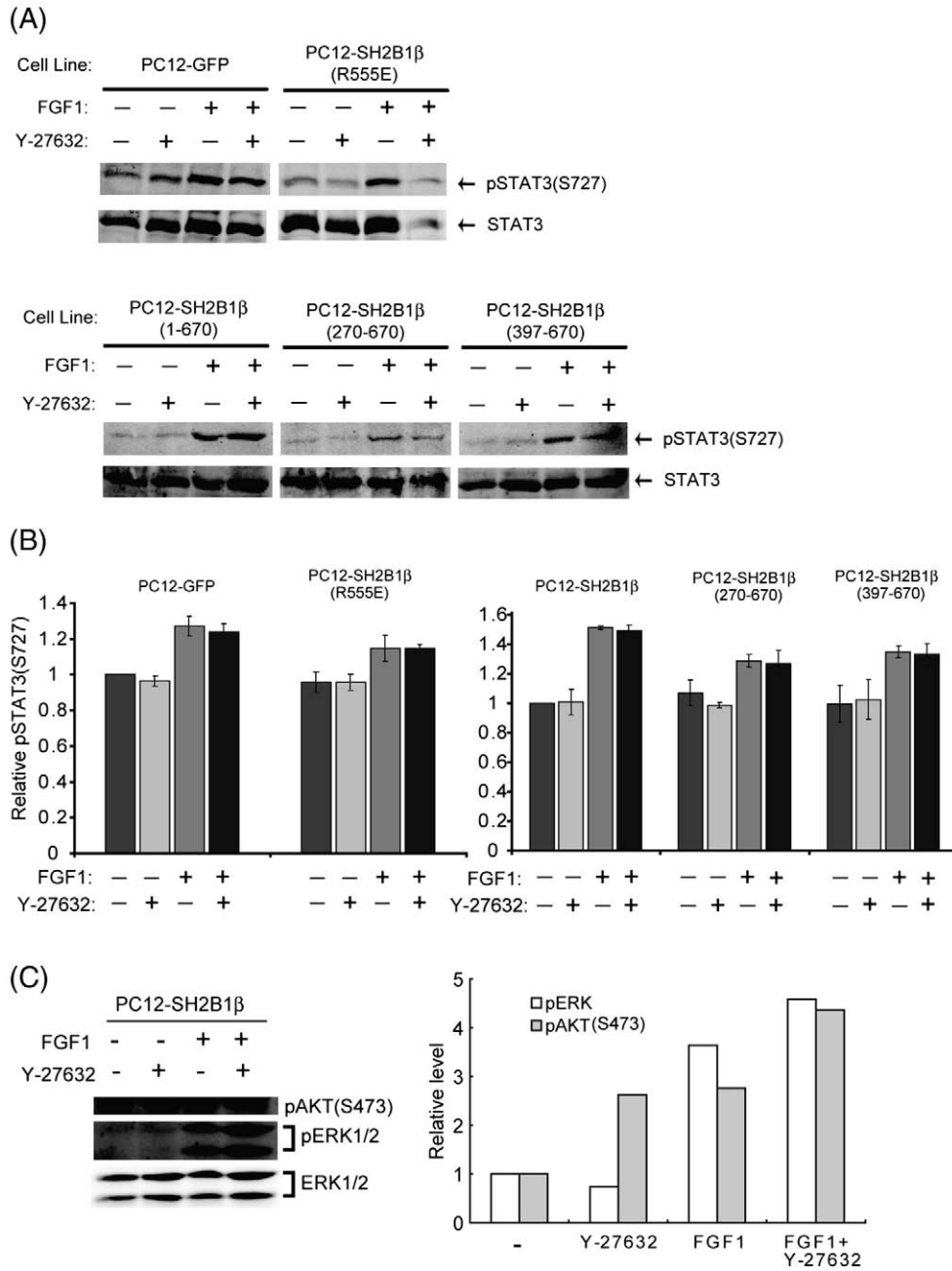
Fig. 11. Inhibiting ROCK does not result in inhibition of FGF1-induced pSTAT3(S727). (A) PC12 cells stably expressing GFP, GFP-SH2B1β, GFP-SH2B1β(R555E), GFP-SH2B1β(270–670) or GFP-SH2B1β(397–670) were stimulated with 100 ng/ml FGF1 for 10 min in the absence or presence of 10 μM ROCK inhibitor, Y-27632. Y-27632 was added 1 h before FGF1 addition. FGF1-induced pSTAT3(S727) was determined via Western blotting. Total STAT3 was used as loading control. (B) Quantified results of the effect of Y-27632 on FGF1-induced pSTAT3(S727) are shown. Data were from three independent experiments. The error bars represent standard errors. (C) PC12-SH2B1β cells were treated without or with 10 μM Y-27632 in the absence or presence of 100 ng/ml FGF1 for 10 min. Y-27632 was added 1 h before FGF1 addition. pAKT(S473) and pERK1/2 levels were determined via Western blotting and ERK1/2 level was used as loading control.

cytoskeleton. In genereal, Rac and Cdc42 promotoe neurite outgrowth while RhoA stimulates retraction [72]. A recent study suggests that combined treatment of ROCK inhibitor and CNTF resulted in enhanced pERK1/2 and pAKT as well as regeneration of retinal ganglion cells [59]. While CNTF induces the tyrosyl phosphorylation of STAT3, the combination of ROCK inhibitor and CNTF reduced the phosphorylation [59]. In contrast, during FGF1-induced neurite outgrowth, we did not detect obvious FGF1-induced tyrosyl phosphorylation of STAT3 (data not shown) suggesting that JAK/STAT pathway is probably not involved. This likely underlies the difference between central and peripheral nervous systems. Interestingly, ROCK inhibition increased

FGF1-induced neurite outgrowth in PC12 cells. We further demonstrated that the increased neurite outgrowth was not due to inhibition of pSTAT3(S727) but likely through increasing pERK1/2 and pAKT. Alternatively, the data may suggest that RhoA inactivation is required for FGF1-induced neurite outgrowth as ROCK is one of the downstream effectors of RhoA.

Taken together, the current study provides the first evidence that the ubiquitously expressed adaptor protein SH2B1β enhances FGF1-induced neurite outgrowth, enhances and prolongs FGF1-induced level of pERK1/2, pAKT and pSTAT3(S727) as well as Egr1 expression in PC12 cells. Moreover, we demonstrate that SH2B1β's enhancement
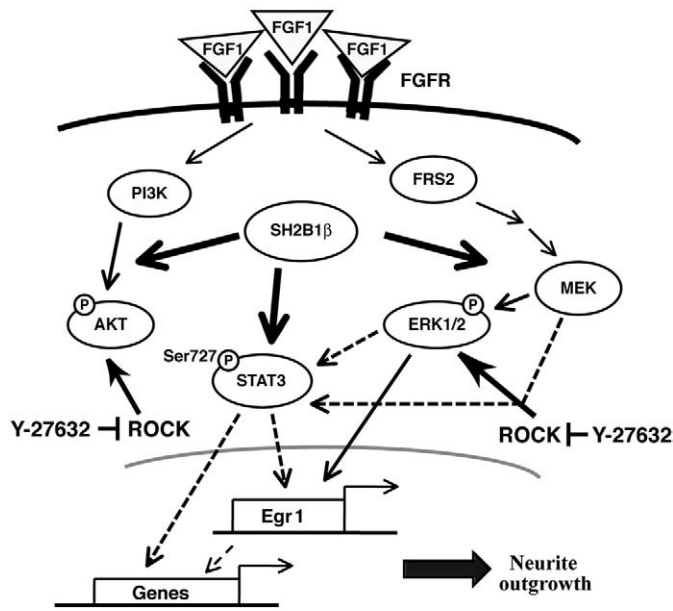
Fig. 12. Working model of how SH2B1β enhances FGF1-induced neurite outgrowth in PC12 cells. SH2B1β enhances and prolongs FGF1-induced MEK-ERK1/2 and PI3K-AKT pathways. SH2B1β also increases pSTAT3(S727) of STAT3 and the expression of Egr1 through MEK-ERK1/2 pathway. Inhibiting ROCK enhances FGF1-induced neurite outgrowth, FGF1-induced pERK1/2 and pAKT but does not affect pSTAT3(S727). Solid line: known pathways or identified pathways in this study. Dashed line: putative steps or involve multiple steps.

on FGF1 signaling and gene expression is largely through MEK-ERK1/2-STAT3-Egr1 pathway. Furthermore, our results suggest that inhibiting ROCK enhances FGF1-induced neurite outgrowth through pSTAT3 (S727)-independent manner.

Acknowledgements

References

[1] T.P. Yamaguchi, J. Rossant, Curr. Opin. Genet. Dev. 5 (4) (1995) 485.
[2] D.M. Ornitz, Cytokine Growth Factor Rev. 16 (2) (2005) 205.
[3] P.J. Marie, J.D. Coffin, M.M. Hurley, J. Cell. Biochem. 96 (5) (2005) 888.
[4] N. Gotoh, K. Manova, S. Tanaka, M. Murohashi, Y. Hadari, A. Lee, Y. Hamada, T. Hiroe, M. Ito, T. Kurihara, H. Nakazato, M. Shibuya, I. Lax, E. Lacy, J. Schlessinger, Mol. Cell. Biol. 25 (10) (2005) 4105.
[5] T.J. Wright, S.L. Mansour, Curr. Top. Dev. Biol. 57 (2003) 225.
[6] T.J. Poole, E.B. Finkelstein, C.M. Cox, Dev. Dyn. 220 (1) (2001) 1.
[7] S. Kato, K. Sekine, Cell. Mol. Biol. (Noisy-le-grand). 45 (5) (1999) 631.
[8] M.C. Naski, D.M. Ornitz, Front. Biosci. 3 (1998) d781.
[9] L. Niswander, C. Tickle, A. Vogel, G. Martin, Mol. Reprod. Dev. 39 (1) (1994) 83 discussion 88-89.
[10] E. Kardami, L. Liu, S. Kishore, B. Pasumarthi, B.W. Doble, P.A. Cattini, Ann. N. Y. Acad. Sci. 752 (1995) 353.
[11] R.E. Rydel, L.A. Greene, J. Neurosci. 7 (11) (1987) 3639.
[12] E. Shi, M. Kan, J. Xu, F. Wang, J. Hou, W.L. McKeehan, Mol. Cell. Biol. 13 (7) (1993) 3907.
[13] N. Su, X. Du, L. Chen, Front. Biosci. 13 (2008) 2842.
[14] J. Partanen, J. Neurochem. 101 (5) (2007) 1185.
[15] B.B. Olwin, K. Arthur, K. Hannon, P. Hein, A. McFall, B. Riley, G. Szebenyi, Z. Zhou, M.E. Zuber, A.C. Rapraeger, et al., Mol. Reprod. Dev. 39 (1) (1994) 90 discussion 100-101.
[16] H. Ohuchi, S. Noji, Cell Tissue Res. 296 (1) (1999) 45.
[17] X. Coumoul, C.X. Deng, Birth Defects Res. C Embryo Today 69 (4) (2003) 286.
[18] L. Chen, C.X. Deng, Front. Biosci. 10 (2005) 1961.
[19] M.B. Goldring, K. Tsuchimochi, K. Ijiri, J. Cell. Biochem. 97 (1) (2006) 33.
[20] S.A. Newman, R. Bhat, Birth Defects Res. C Embryo Today 81 (4) (2007) 305.
[21] E.T. Shifley, S.E. Cole, Birth Defects Res. C Embryo Today 81 (2) (2007) 121.
[22] I.S. Alvarez, M. Araujo, M.A. Nieto, Dev. Biol. 199 (1) (1998) 42.
[23] S.I. Wilson, E. Graziano, R. Harland, T.M. Jessell, T. Edlund, Curr. Biol. 10 (8) (2000) 421.
[24] K.G. Storey, A. Goriely, C.M. Sargent, J.M. Brown, H.D. Burns, H.M. Abud, J.K. Heath, Development 125 (3) (1998) 473.
[25] N. Itoh, Biol. Pharm. Bull. 30 (10) (2007) 1819.
[26] X. Lin, Development 131 (24) (2004) 6009.
[27] W.L. McKeehan, F. Wang, M. Kan, Prog. Nucleic. Acid Res. Mol. Biol. 59 (1998) 135.
[28] W.L. McKeehan, M. Kan, Mol. Reprod. Dev. 39 (1) (1994) 69 discussion 81-62.
[29] D.M. Ornitz, Bioessays 22 (2) (2000) 108.
[30] L. Pellegrini, Curr. Opin. Struct. Biol. 11 (5) (2001) 629.
[31] H. Kouhara, Y.R. Hadari, T. Spivak-Kroizman, J. Schilling, D. Bar-Sagi, I. Lax, J. Schlessinger, Cell 89 (5) (1997) 693.
[32] I. Lax, A. Wong, B. Lamothe, A. Lee, A. Frost, J. Hawes, J. Schlessinger, Mol. Cell 10 (4) (2002) 709.
[33] C. Anneren, C.K. Lindholm, V. Kriz, M. Welsh, Curr. Mol. Med. 3 (4) (2003) 313.
[34] G. Sa, T. Das, Mol. Cell. Biochem. 198 (1-2) (1999) 19.
[35] M.J. Cross, L. Lu, P. Magnusson, D. Nyqvist, K. Holmqvist, M. Welsh, L. Claesson-Welsh, Mol. Biol. Cell 13 (8) (2002) 2881.
[36] M.P. Stavridis, J.S. Lunn, B.J. Collins, K.G. Storey, Development 134 (16) (2007) 2889.
[37] J.G. Heuer, C.S. von Barthheld, Y. Kinoshita, P.C. Evers, M. Bothwell, Neuron 5 (3) (1990) 283.
[38] T. Asai, A. Wanaka, H. Kato, Y. Masana, M. Seo, M. Tohyama, Brain Res. Mol. Brain Res. 17 (1-2) (1993) 174.
[39] N. Yazaki, Y. Hosoi, K. Kawabata, A. Miyake, M. Minami, M. Satoh, M. Ohta, T. Kawasaki, N. Itoh, J. Neurosci. Res. 37 (4) (1994) 445.
[40] K. Peters, D. Ornitz, S. Werner, L. Williams, Dev. Biol. 155 (2) (1993) 423.
[41] H. Riedel, J. Wang, H. Hansen, N. Yousaf, J. Biochem. 122 (6) (1997) 1105.
[42] L. Rui, L.S. Mathews, K. Hotta, T.A. Gustafson, C. Carter-Su, Mol. Cell Biol. 17 (11) (1997) 6633.
[43] N. Yousaf, Y. Deng, Y. Kang, H. Riedel, J. Biol. Chem. 276 (44) (2001) 40940.
[44] L. Rui, J. Herrington, C. Carter-Su, J. Biol. Chem. 274 (15) (1999) 10590.
[45] X. Qian, A. Riccio, Y. Zhang, D.D. Ginty, Neuron 21 (5) (1998) 1017.
[46] X. Qian, D.D. Ginty, Mol. Cell. Biol. 21 (5) (2001) 1613.
[47] L. Chen, C. Carter-Su, Mol. Cell. Biol. 24 (9) (2004) 3633.
[48] L. Chen, T.J. Maures, H. Jin, J.S. Huo, S.A. Rabbani, J. Schwartz, C. Carter-Su, Mol. Endocrinol. 22 (2) (2008) 454.
[49] Y. Zhang, W. Zhu, Y.G. Wang, X.J. Liu, L. Jiao, X. Liu, Z.H. Zhang, C.L. Lu, C. He, J. Cell. Sci. 119 (Pt 8) (2006) 1666.
[50] R.E. Rydel, L.A. Greene, J. Neurosci. 7 (11) (1987) 3639.
[51] D.H. Damon, P.A. D'Amore, J.A. Wagner, J. Cell. Physiol. 135 (2) (1988) 293.
[52] P. Claude, I.M. Parada, K.A. Gordon, P.A. D'Amore, J.A. Wagner, Neuron 1 (9) (1988) 783.
[53] F. Renaud, S. Desset, L. Oliver, G. Gimenez-Gallego, E. Van Obberghen, Y. Courtois, M. Laurent, J. Biol. Chem. 271 (5) (1996) 2801.
[54] Y.P. Ng, Z.H. Cheung, N.Y. Ip, J. Biol. Chem. 281 (23) (2006) 15636.
[55] M. Nikolic, H. Dudek, Y.T. Kwon, Y.F. Ramos, L.H. Tsai, Genes Dev. 10 (7) (1996) 816.
[56] A.K. Fu, W.Y. Fu, A.K. Ng, W.W. Chien, Y.P. Ng, J.H. Wang, N.Y. Ip, Proc. Natl. Acad. Sci. U. S. A. 101 (17) (2004) 6728.
[57] N.Y. Ip, J. McClain, N.X. Barrezueta, T.H. Aldrich, L. Pan, Y. Li, S.J. Wiegand, B. Friedman, S. Davis, G.D. Yancopoulos, Neuron 10 (1) (1993) 89.
[58] J. Mey, S. Thanos, Brain Res. 602 (2) (1993) 304.
[59] P. Lingor, L. Tonges, N. Pieper, C. Bermel, E. Barski, V. Planchamp, M. Bahr, Brain 131 (Pt 1) (2008) 250.
[60] K. Kotani, P. Wilden, T.S. Pillay, Biochem. J. 335 (Pt 1) (1998) 103.
[61] L. Rui, C. Carter-Su, J. Biol. Chem. 273 (33) (1998) 21239.
[62] M. Kong, C.S. Wang, D.J. Donoghue, J. Biol. Chem. 277 (18) (2002) 15962.
[63] J.J. O'Shea, M. Gadina, R.D. Schreiber, Cell 109 (2002) S121 Suppl.
[64] W.J. Leonard, Int. J. Hematol. 73 (3) (2001) 271.
[65] M.H. Heim, J. Recept. Signal. Transduct. Res. 19 (1–4) (1999) 75.
[66] K.D. Liu, S.L. Gaffen, M.A. Goldsmith, Curr. Opin. Immunol. 10 (3) (1998) 271.
[67] N.C. Reich, Cytokine Growth Factor Rev. 18 (5–6) (2007) 511.
[68] J.J. Schuringa, H. Schepers, E. Vellenga, W. Kruijer, FEBS Lett. 495 (1–2) (2001) 71.
[69] W. Sun, M. Snyder, D.E. Levy, J.J. Zhang, FEBS Lett. 580 (25) (2006) 5880.
[70] L. Gautron, V. De Smedt-Peyrusse, S. Laye, Brain Res. 1098 (1) (2006) 26.
[71] Z. Li, M.H. Theus, L. Wei, Dev. Growth Differ. 48 (8) (2006) 513.
[72] C.G. Koh, Neurosignals 15 (5) (2006) 228.